CrystEngComm

Accepted Manuscript

ROYAL SOCIETY OF CHEMISTRY

www.rsc.org/crystengcomm

Journal Name

RSCPublishing

ARTICLE

Structural diversity and magnetic properties of three metal−organic frameworks assembled from a T-shaped linker

Cite this: DOI: 10.1039/x0xx00000x

Received 00th January 2012,
Accepted 00th January 2012

DOI: 10.1039/x0xx00000x

www.rsc.org/

Jing Wang,[a] Xuemin Jing,[b] Yu Cao,[a] Guanghua Li,[a] Qisheng Huo[a] and Yunling Liu*[a]

Three metal-organic frameworks, [Mn(bpydc)]·DMA (**JLU-Liu11**), [Co(bpydc)DMSO]·(DMSO)(H_2O) (**JLU-Liu12**) and [Co(bpydc)H_2O]·H_2O (**JLU-Liu13**), have been solvothermally synthesized by reacting a T-shaped linker, 2,2′-bipyridyl-5,5′-dicarboxylic acid (H_2bpydc) ligand with transition metals. These compounds exhibit three different types of structures. In **JLU-Liu11**, two oxygen atoms and two nitrogen atoms of the H_2bpydc ligand coordinate to five manganese centers to form an **ant** net, and **JLU-Liu11** displays two types of helical chains with opposite helical directions, which are composed of vertex-sharing 4-rings propagating along [100] direction. In **JLU-Liu12**, H_2bpydc ligands coordinate to cobalt centers to form a new (3, 3)-connected net with two different tiles (6.12^4) and ($6^2.12^6$). In **JLU-Liu13**, H_2bpydc ligands coordinate to cobalt centers to form a two-dimensional layer which then interact with terminal water molecules via hydrogen bonds to construct a three-dimensional supramolecular structure, **JLU-Liu13** shows exceptional stability in water. Additionally, the magnetic properties of all compounds have been studied.

Introduction

Design and synthesis of metal-organic frameworks (MOFs) have attracted much attention for their interesting structural topologies[1] and extensive potential applications as functional materials, such as catalysis,[2] nonlinear optics,[3] magnetism,[4] luminescence,[5] chirality,[6] chemical sensors,[7] gas sorption[8] and so on. The rapid growth of crystal engineering is inevitable to comprise the rational design and preparation of crystalline material with novel topologies and desired functions. Generally, the synthesis of MOFs depends on several factors, such as the metal atoms, organic ligands, temperature, pH value, solvent and et al.[9] It is found that the selection of metal ions and organic linkers is very important for the final structures and properties of MOFs. Among multifarious metal ions, transition metals manifest a wide variety of coordination modes and geometries, which are helpful in the formation of novel MOFs with varied structural topologies and properties.[10] To date, MOFs based on transition metals exhibit various structural motifs, such as one dimensional (1D) chains, two dimensional (2D) grids and three dimensional (3D) porous structures,[11] which display interesting properties. On the other hand, the main rational synthetic strategy has been focused on the use of a suitable organic ligand in directing the construction of MOFs with desirable structures and properties, and much attention has been devoted to choose or design various multifunctional bridging ligands.[12]

Recently, the N-heterocyclic carboxylate ligand, for instance, 2,2′-bipyridyl-5,5′-dicarboxylic acid (H_2bpydc),[13] has gained considerable attention due to its abundant coordination modes and functional properties. The H_2bpydc ligand displays two main coordinated modes: (1) linear mode, two nitrogen donors of the 2,2-bipyrine group open or load metal ions such as Pd, Ir, Ru and Cu ions; (2) T-shaped mode, all coordination sites linked with metal centers. To the best of our knowledge, T-shaped linkers usually give rise to chiral / helical structures due to its flexible rotating properties, which have been investigated in other T-shaped ligand such as 4,5-imidazoledicarboxylic acid and its derivatives.[14] Inspired by this, we select H_2bpydc as a T-shaped linker to coordinate with transition metals to generate helical structures.

In this paper, as a continuation of our previous work,[13h, i] we used H_2bpydc ligand as a T-shaped linker to react with different metal centers (Mn and Co), and successfully synthesized three novel MOFs, namely [Mn(bpydc)]·DMA (**JLU-Liu11**), [Co(bpydc)DMSO]·(DMSO)(H_2O) (**JLU-Liu12**) and [Co(bpydc)H_2O]·H_2O (**JLU-Liu13**), which exhibited diverse structures and typical antiferromagnetic properties. Meanwhile,

the structures, infrared spectra (IR), elemental analyses, powder X-ray diffraction (PXRD), magnetic properties, and thermogravimetric analyses (TGA) were explored in detail.

Experimental

Materials and methods

All chemicals were obtained from commercial sources and used without further purification. Powder X-ray diffraction (XRD) data were collected on a Rigaku D/max-2550 diffractometer with Cu Kα radiation (λ = 1.5418 Å). Elemental analyses (C, H, and N) were achieved by vario MICRO (Elementar, Germany). Infrared (IR) spectra were recorded within a 400-4000 cm^{-1} region on a Nicolet Impact 410 FTIR spectrometer with KBr pellets. The thermal gravimetric analyses (TGA) were performed on TGA Q500 thermogravimetric analyzer used in air with a heating rate of 10 ^{o}C min^{-1}. Variable-temperature magnetic susceptibility data were obtained with SQUID magnetometer (Quantum Design, MPMS-5) in the temperature range 2-300 K by using an applied field of 1000 Oe.

Synthesis of JLU-Liu11

A mixture of $Mn(NO_3)_2$ (50% aqueous solution) (0.014 g, 0.04 mmol), H_2bpydc (0.0025 g, 0.01 mmol), 4,4′-trimethylenedipiperidine (0.05 mL, 0.95 M in H_2O), HNO_3 (0.1 mL, 2.8 M in N,N-dimethylacetamide (DMA)), DMA (1 mL) and N,N-dimethylformamide (DMF) (0.5 mL) was added, respectively, into a 20 mL vial. And then the vial was sealed and kept at 85 °C for 12 h and 105 °C for another 24 h. Colorless octahedral crystals were collected and dried in the air (58% yield based on $Mn(NO_3)_2$). Elemental analysis (wt %) for **JLU-Liu11**: calcd: C, 50.01; H, 3.934; N, 10.94. found: C, 50.15; H, 4.061; N, 10.96.

Synthesis of JLU-Liu12

A mixture of $Co(NO_3)_2{\cdot}6H_2O$ (0.012 g, 0.04 mmol), H_2bpydc (0.0025 g, 0.01 mmol), morpholine (0.05 mL, 2.3 M in DMF) and dimethylsulfoxide (DMSO) (1 mL) was added, respectively, into a 20 mL vial. And then the vial was sealed and kept at 85 °C for 18 h. Red cubic crystals were collected and dried in the air (85 % yield based on $Co(NO_3)_2{\cdot}6H_2O$). Elemental analysis (wt %) for **JLU-Liu12**: calcd: C, 40.42; H, 4.240; N, 5.892; S, 13.49. found: C, 39.24; H, 3.985; N, 5.830; S, 13.33.

Synthesis of JLU-Liu13

A mixture of $Co(CH_3COO)_2{\cdot}4H_2O$ (0.010 g, 0.04 mmol), H_2bpydc (0.0025 g, 0.01 mmol), HNO_3 (0.3 mL, 2.8 M in DMF), DMF (0.5 mL), H_2O (0.5 mL) and CH_3CN (0.5 mL) was added, respectively, into a 20 mL vial. And then the vial was sealed and kept at 85 °C for 18 h. Pink crystals were collected and dried in the air (40% yield based on $Co(CH_3COO)_2{\cdot}4H_2O$). Elemental analysis (wt %) for **JLU-Liu13**: calcd: C, 42.75; H, 2.989; N, 8.309. found: C, 42.24; H, 2.635; N, 3.055.

X-ray Crystallography

Crystallographic data for **JLU-Liu11-13** were collected on a Bruker Apex II CCD diffractometer using graphite-monochromated Mo-*K*α (λ = 0.71073 Å) radiation at room temperature. The structures were solved by direct methods and refined by full-matrix least-squares on F^2 using version 5.1.[15] All the metal atoms were located first, and then the oxygen and carbon atoms of the compounds were subsequently found in difference Fourier maps. The hydrogen atoms of the ligand were placed geometrically. All non-hydrogen atoms were refined anisotropically. The final formulas (**JLU-Liu11**, **12)** were derived from crystallographic data combined with elemental and thermogravimetric analysis data. Crystallographic data for **JLU-Liu11-13** (1003340-1003342) have been deposited with Cambridge Crystallographic Data Centre. Data can be obtained free of charge upon request at www.ccdc.cam.ac.uk/data_request/cif. Crystal data and detailed data collection and refinement of **JLU-Liu11-13** are summarized in Table 1. Topology information for **JLU-Liu11-13** was calculated by TOPOS 4.0.[16]

Table 1 Crystal data and structure refinement for **JLU-Liu11**, **JLU-Liu12** and **JLU-Liu13**

compound	JLU-Liu11	JLU-Liu12	JLU-Liu13
formula	$C_{16}H_{15}MnN_3O_5$	$C_{16}H_{20}CoN_2O_7S_2$	$C_{12}H_{10}CoN_2O_6$
fw	384.25	475.39	337.15
temp (K)	296(2)	293(2)	296(2)
crystal system	orthorhombic	cubic	monoclinic
space group	*Fddd*	*Pa*-3	$P2_1/n$
a (Å)	17.0010(19)	24.755(3)	11.9082(10)
b (Å)	19.633(2)	24.755(3)	8.3277(7)
c (Å)	23.109(4)	24.755(3)	12.7165(11)
α (°)	90	90	90
β (°)	90	90	97.361(2)
γ (°)	90	90	90
V (Å^3)	7713.5(19)	15170(3)	1250.68(18)
Z	16	24	4
Dc (Mg/m^3)	1.324	1.246	1.791
μ(mm^{-1})	0.712	0.876	1.404
F(000)	3152	5880	684
Reflections collected	11352/2391	93505/4496	7683/2228
Unique (Rint)	[R(int) = 0.0547]	[R(int) = 0.1166]	[R(int) = 0.0160]
Goodness on fit	1.105	1.078	1.095
R_1, wR_2 [$I>2\sigma(I)$]	0.0750, 0.2098	0.0885, 0.2191	0.0264, 0.0714
R_1, wR_2 (all data)	0.1079, 0.2325	0.1350, 0.2466	0.0278, 0.0724

Results and discussion

Structure description of compound JLU-Liu11

Single-crystal X-ray diffraction analysis reveals that **JLU-Liu11** crystallizes in the orthorhombic crystal system with space group of *Fddd*. The asymmetric unit of **JLU-Liu11**

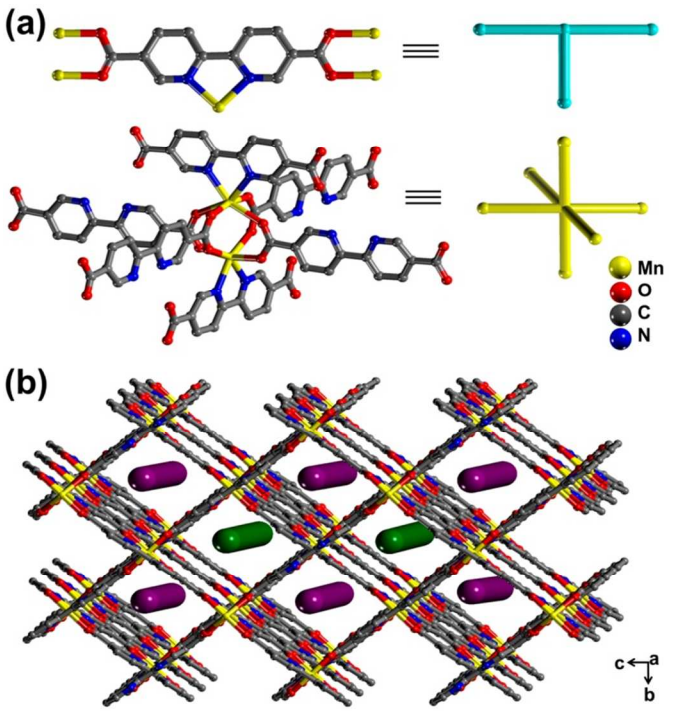

Fig. 1 (a) Description of the structure of **JLU-Liu11**: illustration of the ligand and dinuclear Mn (II) units, viewed as a (3, 6)-connected nodes; (b) View of channels with helical channels along the [100] direction (green stick: left chains, purple stick: right chains).

consists of one crystallographically independent Mn(II) atom, one ligand molecule. The Mn atoms display distorted octahedral [MnN_2O_4] geometries with two nitrogen and four oxygen atoms from five individual ligands (Fig. 1a). The Mn1 atom lies on a twofold axis which also passes through the mid-point of the C-C bond linking the two pyridyl rings in the 2,2′-bipyridyl-5,5′-dicarboxylate ligand. Two adjacent Mn1 atoms are bridged by oxygen atoms from carboxyl groups to form a dinuclear building unit (Fig. S1a†). The Mn-O and Mn-N bond distances are in the range of 2.041(3)-2.348(3) Å and 2.30(3)-2.37(3) Å, respectively. It is noteworthy that the H_2bpydc ligand shows bidentate bridging coordination mode and coordinates with five Mn atoms.

It is interesting to note that **JLU-Liu11** exhibits two types of helical chains with opposite helical directions (left- and right-handed) (Fig. 1b, Fig. 2a). In the structure of **JLU-Liu11**, the (3, 6)-connected net consists of infinite helical vertex-sharing 4-ring chains. The adjacent angles in a parallelogram are 85.14 and 94.85° (metal-ligand-metal, ligand-metal-ligand), respectively. Two independent 4-ring chains share vertex to form 1D channels along the [100] direction (Fig. S1b†). Additionally, both helical channels can be viewed as two independent 4-ring chains arranged in an anticlockwise / clockwise direction with dihedral angle about 81.18 and 99.65° to generate two helical chains with a pitch of 17 Å corresponding to the length of the *a* axis (Fig. 2b).

The 3D framework exhibits three types of open channels along different directions. One type of channel with a

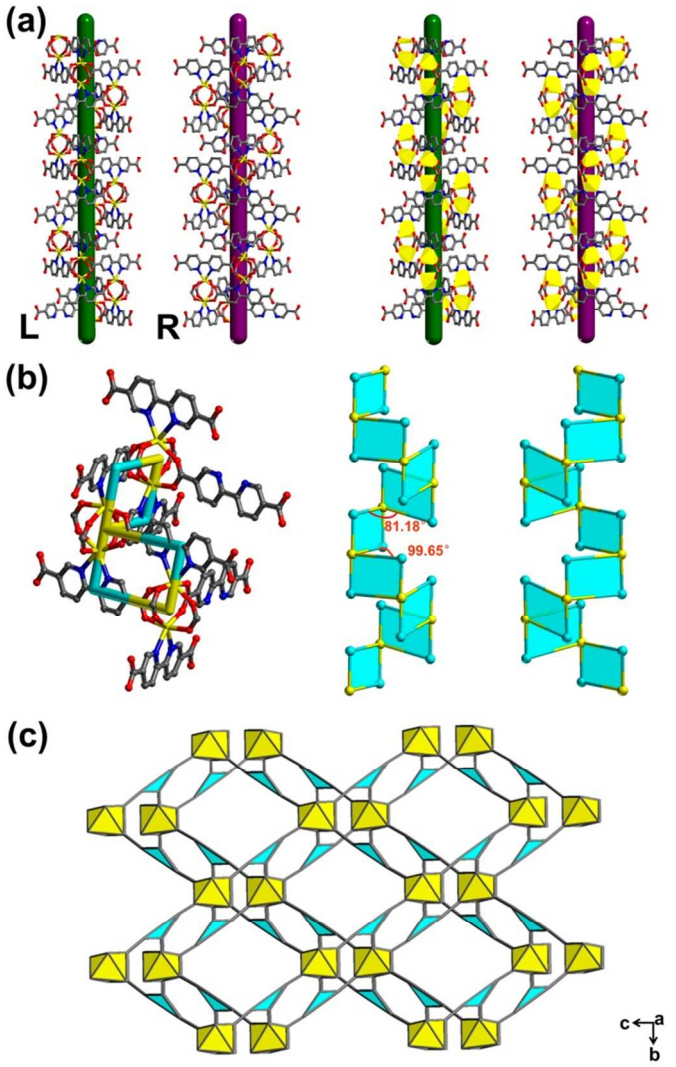

Fig. 2 (a) Two types of helical chains; (b) Characteristics of helical chains; (c) **ant** network with open channels along the [100] direction.

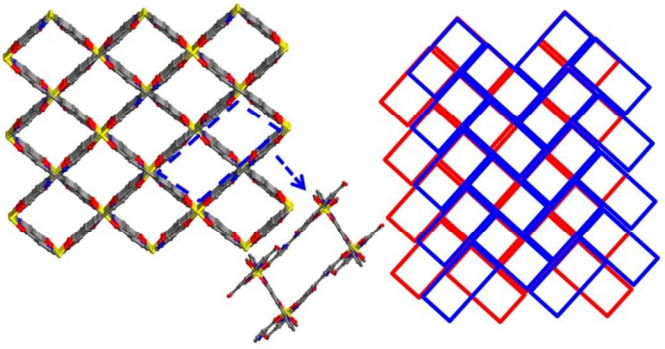

Fig. 3 View along the *a* axis, along with a representation of two adjacent layers; each has a herringbone arrangement of rectangular pores; one such rectangular subunit is shown, lower middle.

quadrangle shape has the openings with an approximate diameter of 4.9×11.7 Å along the *a* axis. Within a layer perpendicular to the *a* axis, the pores are arranged in a herringbone fashion, but the adjacent layers are stacked along

the *a* axis in such a way that the pattern appears to have four-fold symmetry in projection (Fig. 3), and similar networks have been reported.[13c, 13h, 17] Topologically, the ligand links to three dinuclear Mn building units and can be regarded as a 3-connected node, the dinuclear Mn building units link to six organic ligands and can be viewed as a 6-connected node. Thus, the 3D framework of **JLU-Liu11** can be described as a (3, 6)-connected net with **ant** topology[18] (Fig. S1b†), which possesses two different tiles (8^3) and ($4^2.8^2$) with the vertex symbol of $4.4.8^{10}$. PLATON[19] analysis reveals that the 3D porous structure has a solvent area volume of 4243 Å^3, which represents 55% per unit cell volume.

Structure description of compound JLU-Liu12

Single-crystal X-ray diffraction analysis reveals that **JLU-Liu12** crystallizes in the cubic crystal system with space group of *Pa*-3. The asymmetric unit of **JLU-Liu12** consists of one Co atom, one ligand molecule, and one dimethylsulfoxide molecule (DMSO) (Fig. 4a). Co atoms form distorted octahedral [CoN_2O_4] geometries with two nitrogen and three oxygen atoms from three individual ligands and one oxygen atom from DMSO (Fig. S2a†). The Co-O and Co-N bond distances lie in the range of 1.974(11)-2.311(5) Å and 2.097(5)-2.112(5) Å, respectively The H_2bpydc ligand displays monodentate and bidentate bridging coordination modes and coordinates with three Co atoms.

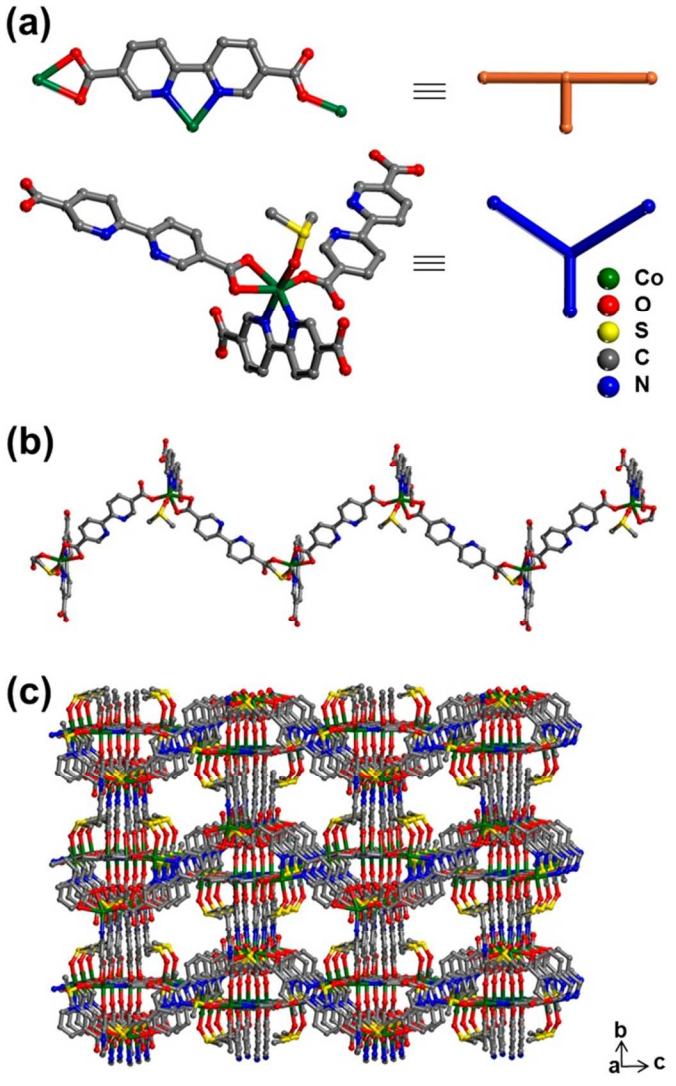

Fig. 4 (a) Description of the structure of **JLU-Liu12**: illustration of the ligand and Co (II) units, viewed as a (3, 3)-connected nodes; (b) 1D zigzag chain; (c) The 3D framework is constructed by 1D zigzag chains.

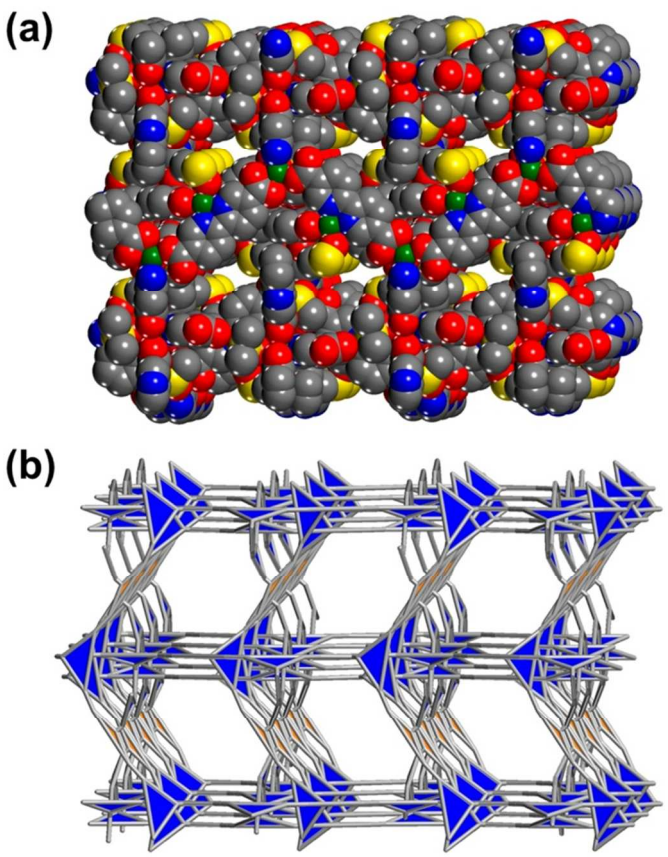

Fig. 5 (a) Space-filling representation of the 3D framework; (b) A network with open channels along the [001] direction.

In the **JLU-Liu12**, $bpydc^{2-}$ anions connect Co(II) ions to generate 1D zigzag chains (Fig. 4b). The zigzag chains link each other to form a 3D network (Fig. 4c), and the opening size of the channel is about 4.2×4.2 Å (Fig. 5a). The interesting feature of the structure is there existing helical chains. Co centers are interconnected by a bridging ligand to form 1D infinite left / right helical chains of $[Co\text{-}bpydc]_n$ running along the [111] direction (Fig. S2c†), and the left / right helical chains exist alternately (Fig. S2d†).

To further understand the structure, topological analysis is performed on **JLU-Liu12**. H_2bpydc can be viewed as a 3-connected node, and Co also can be regarded as a 3-connected node. Such connectivity repeats infinitely to generate a new (3, 3)-connected topology (Fig. 5b). And the compound possesses two different tiles (6.12^4) and ($6^2.12^6$) with point symbol of 6.12^2. PLATON analysis reveals that the 3D porous structure has a solvent area volume of 7580 Å^3, which represents 50% per unit cell volume.

Structure description of compound JLU-Liu13

Single-crystal X-ray diffraction analysis reveals that **JLU-Liu13** crystallizes in the monoclinic crystal system with space group of $P2_1/n$. The asymmetric unit of **JLU-Liu13** consists of one Co atom, one ligand molecule, and one terminal water molecule (Fig. 6a). The Co atoms display distorted octahedral [CoN_2O_4] geometries with two nitrogen and three oxygen atoms from three individual ligands and one oxygen atom from water molecule (Fig. S3a†). Similarly to **JLU-Liu12**, the Co center and H_2bpydc ligand in **JLU-Liu13** can be viewed as a 3-connected node as well (Fig. 6b). It is a new 2-dimensional layer topology. The point symbol for **JLU-Liu13** is $8^2.10$. The Co-O and Co-N bond distance lie in the range of 2.032(16)-2.218(16) Å and 2.099(17)-2.109(17) Å, respectively. The H_2bpydc ligand exhibits monodentate and bidentate bridging coordination modes and coordinates with three Co atoms.

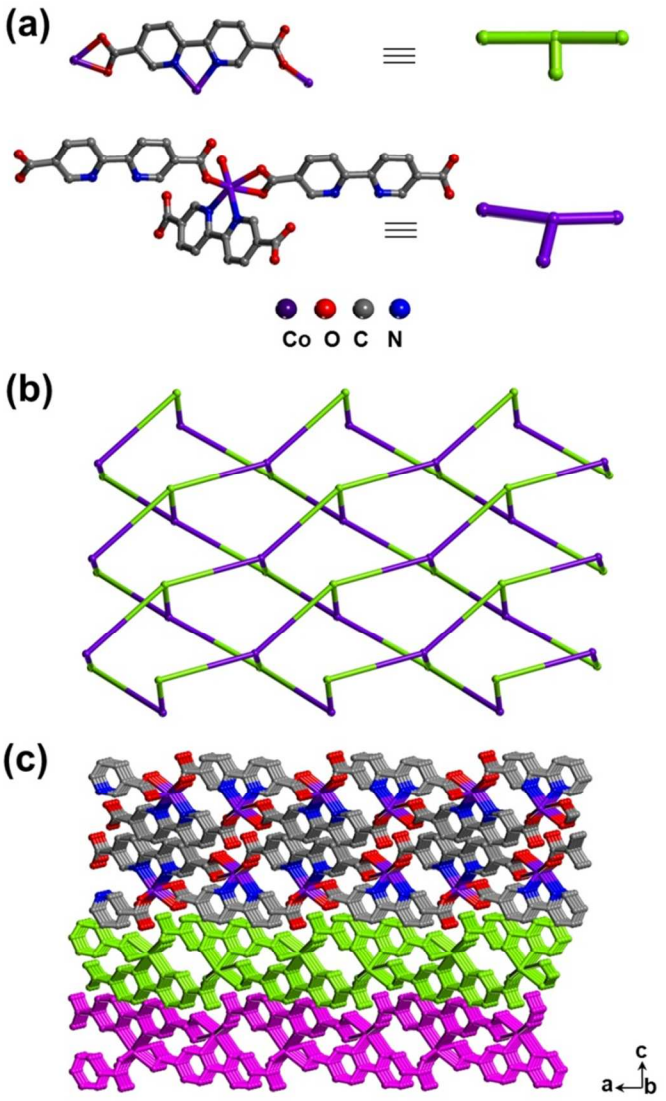

Fig. 6 (a) Description of the structure of **JLU-Liu13**: illustration of the ligand and Co (II) units, viewed as a (3, 3)-connected nodes; (b) 3-connected inorganic SBUs and 3-connected organic SBUs connect to form a layered (3, 3)-network; (c) Stacking pattern of 2D framework along the [010] direction.

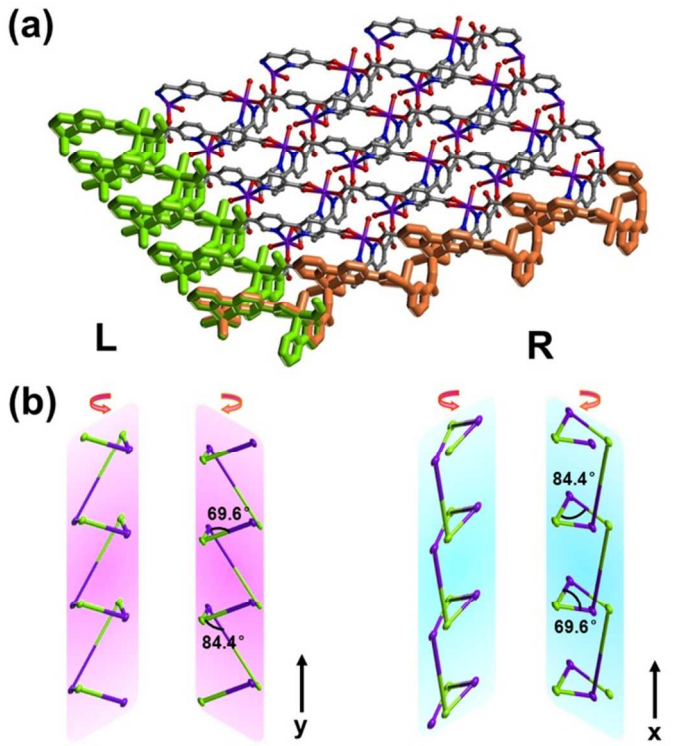

Fig. 7 (a) Two kinds of helical chains on one layer; (b) Two types of helical chains on adjacent two layers along the same axis.

In the **JLU-Liu13**, the H_2bpydc ligand is linked with three Co centers to form a 2D framework (Fig. 6c). The adjacent layers adopt an ABAB stacking, which lead to the formation of smaller rhombus channels. As show in Fig.7a, in the identical layer, there exists 1D left- and right-handed helical chain along different axis directions. It is interesting to note that left- and right-handed helical chains vertically exist on one layer. Both the helical channels can be viewed as {metal···ligand···metal} arranged in an anticlockwise / clockwise direction with different torsion angles about 69.6 and 84.4° to generate two helical chains with the pitches of 8.3 and 11.9 Å. And more interesting, **JLU-Liu13** exhibits two types of helical chains with opposite helical directions on adjacent two layers along the same axis (Fig. 7b, S3b†).

The neighboring 2D layers with 1D channel are further assembled into a 3D supramolecular architecture, through hydrogen bonds between the terminal water molecule and the carboxylate oxygen atoms (Fig. S3c†, d†). PLATON analysis reveals that the structure has a solvent area volume of 171.2 $Å^3$, which represents 13% per unit cell volume.

From the above description and discussion, the diverse solvents also have a great influence on the construction of the three different compounds. When the temperature of reaction is about 85 ^oC and the ratio of metal to ligand is about 4:1, the final structure of the compound is determined by the kinds of solvents. For instance, **JLU-Liu12** is obtained by utilizing the pure DMSO as the solution and it manifests 3D (3, 3)-connected topology. When DMF, ethanol and H_2O as the mixed solvents, **JLU-Liu13** is gained and displays 2D (3, 3)-

connected topology. In the **JLU-Liu12** and **JLU-Liu13**, although both of metal center and ligand can be regarded as a 3-connected node, the angles are completely different in the 3-connected simplified structures (Fig. S5†). It may be the reason that the distinct structures are formed in two compounds.

Recently, our group is focused on the design and synthesis of MOFs based on the H_2bpydc ligand. The synthetic methods for MOFs or coordination polymers (CPs) are easily affected by several factors, such as the ratio of metal and ligand, metal ions, solvent polarity and so on, which can influence the formation of the final structures. Considering these factors, we have successfully synthesized eight new MOFs with novel topologies [13h, i] by rational design of reaction conditions, such as controlling the relative molar ratio of metals and the H_2bpydc ligand, selecting different metal sources, anions and solvents. The synthetic routes of eight compounds based on different metal sources and H_2bpydc ligand have been shown in Scheme S1†. These compounds with different topologies, such as **ant**, **ung**, **crb**, **cbo** and new topology, exhibit interesting gas adsorption, luminescence and magnetic properties. Therefore, the rational design and preparation of CPs or MOF materials with desired topologies and properties is crucial.

The coordination chemistry of H_2bpydc is interesting, since its two carboxylate groups can be easy fully deprotonated to generate $bpydc^{2-}$ anions under different synthesis conditions. The deprotonated $bpydc^{2-}$ anions often adopt monodentate and bidentate bridging coordination modes. In addition, two nitrogen donors of the 2,2-bipyrine group may be opened or loaded. Therefore, it can coordinate with metal ions in variety ways to form a series of novel coordination polymers with interesting topologies and properties. Combined with above structural analysis, the structural diversities in three compounds maybe directly benefit from the versatile coordination modes of $bpydc^{2-}$ anions, which may link metal centers in many coordination modes, and we just give a few examples here (Scheme 1). Among these modes, two new coordination modes have been explored in this paper; mode (c) appears in **JLU-Liu11**, while mode (j) is observed in **JLU-Liu12** and **JLU-Liu13**, respectively.

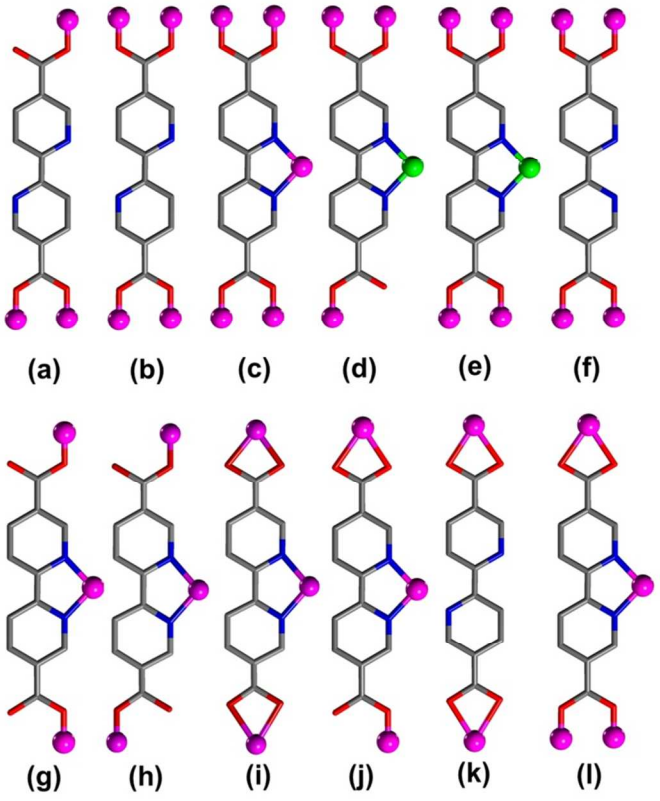

Scheme 1 Several coordination modes of the H_2bpydc ligand (a)-(l). Color scheme: carbon, gray; nitrogen, blue; oxygen, red; metal, green and pink.

Thermogravimetric Analysis

As shown in Fig. S7†, the TG analysis curve for **JLU-Liu11** shows a weight loss of 17 % between 30 and 170 °C, which corresponds to the loss of the DMA molecules. Upon further heating, a weight loss of 63 % between 170 and 450 °C occurs due to the collapse of the framework (calcd: 65%). PXRD studies indicated that the final product, upon calcinations above 450 °C, is a main phase of Mn_2O_3 (JCPDS: 41-1442).

The TG analysis curve for **JLU-Liu12** shows a weight loss of 20 % between 30 and 150 °C, which corresponds to the loss of the DMSO and H_2O molecules. Upon further heating, a weight loss of 65% between 150 and 500 °C occurs due to the collapse of the framework (calcd: 67 %). PXRD studies indicated that the final product, upon calcinations above 500 °C, is a main phase of Co_3O_4 (JCPDS: 43-1003).

The TG analysis curve for **JLU-Liu13** shows a weight loss of 11 % between 30 and 230 °C, which corresponds to the loss of the H_2O molecules. Upon further heating, a weight loss of 65% between 230 and 400 °C occurs due to the collapse of the framework (calcd: 70 %). PXRD studies indicated that the final product, upon calcinations above 400 °C, is a main phase of Co_3O_4 (JCPDS: 43-1003).

Stability

The as-synthesized samples are immersed in acetonitrile, dichloromethane, methanol and ethanol solvent for 48h at room temperature, the TGA curves show that guest molecules have been successfully exchanged. However, the PXRD of **JLU-Liu11** and **JLU-Liu12** indicate that the frameworks can't keep their crystallinity after the guest molecules are removed (Fig. S8†). Although **JLU-Liu11** and **JLU-Liu12** have the big pores for N_2 adsorption, they do not adsorb N_2 at 77K due to the low stability after evacuation. The PXRD of **JLU-Liu13** shows that the framework can keep their stability after immersed in distinct solvents (Fig. S9†). Furthermore, the stability of **JLU-Liu13** is unchanged on standing for a week in water (Fig. 8). It is well known that most MOFs are unstable in water. However, **JLU-Liu13** stacks parallel each other in an ABAB accumulation which has the small pores (Fig. S10c†), it does not adsorb CO_2 and N_2.

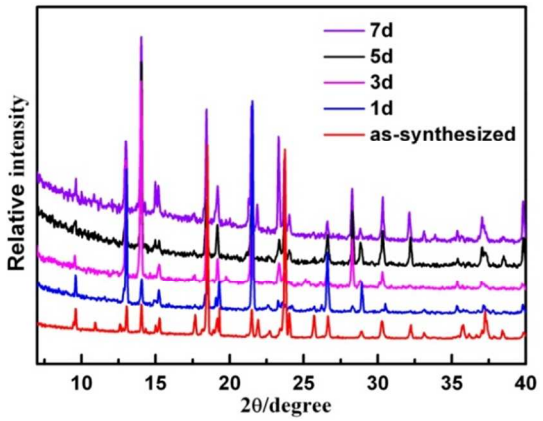

Fig. 8 The PXRD patterns of **JLU-Liu13** after immersed in H_2O.

Magnetic Properties

Magnetic susceptibility of **JLU-Liu11-13** is measured in an applied field of 1 kOe for the samples over the temperature range of 2-300 K, as shown in Fig. 9. The $\chi_M T$ value for **JLU-Liu11** is 3.47 cm^3 K mol^{-1} at 300 K. On cooling, $\chi_M T$ decreases rapidly down to 0.038 cm^3 K mol^{-1} at 2 K. The magnetic susceptibility from 2 to 300 K obeys the Curie-Weiss law [$\chi_M = C/(T - \theta)$] with a Weiss constant θ of -25.33 K and a Curie constant C of 3.764 cm^3 K mol^{-1}. The $\chi_M T$ value for **JLU-Liu12** is 3.832 cm^3 K mol^{-1} at 300 K. On cooling, $\chi_M T$ decreases rapidly down to 1.719 cm^3 K mol^{-1} at 2 K. The magnetic susceptibility from 2 to 300 K obeys the Curie-Weiss law [$\chi_M = C/(T - \theta)$] with a Weiss constant θ of -20.38 K and a Curie constant C of 3.787 cm^3 K mol^{-1}. The $\chi_M T$ value for **JLU-Liu13** is 4 cm^3 K mol^{-1} at 300 K. On cooling, $\chi_M T$ decreases rapidly down to 1.855cm^3 K mol^{-1} at 2 K. The magnetic susceptibility from 2 to 300 K obeys the Curie-Weiss law [$\chi_M = C/(T - \theta)$] with a Weiss constant θ of -22.67 K and a Curie constant C of 4.213 cm^3 K mol^{-1}. Consequently, all of the compounds show typical antiferromagnetic character.

Conclusions

In summary, 2,2′-bipyridyl-5,5′-dicarboxylic acid can be simplified as a 3-connected T-shaped linker, chelating with M^{2+} atoms (M = Mn^{2+} and Co^{2+}) to construct two 3D frameworks and one 2D structure with various topologies and single-helical chains. In **JLU-Liu11**, metal atoms are connected with ligand to form quadrangle channels, and the typically structural feature of compound is the infinite helical vertex-sharing 4-ring chains. The zigzag chains link each other to form compound **JLU-Liu12** with interesting helical chains, which exhibits a new topology. The feature of **JLU-Liu13** is single-helical arrangement of the framework and water stability. The successful isolation of three materials not only affords novel compounds with interesting structures but also helps us to further understand the essence of helix characters. The structural diversity of secondary building units (SBUs) brings illustrious magnetic behaviors in these compounds. Further research around this area is on-going in our group.

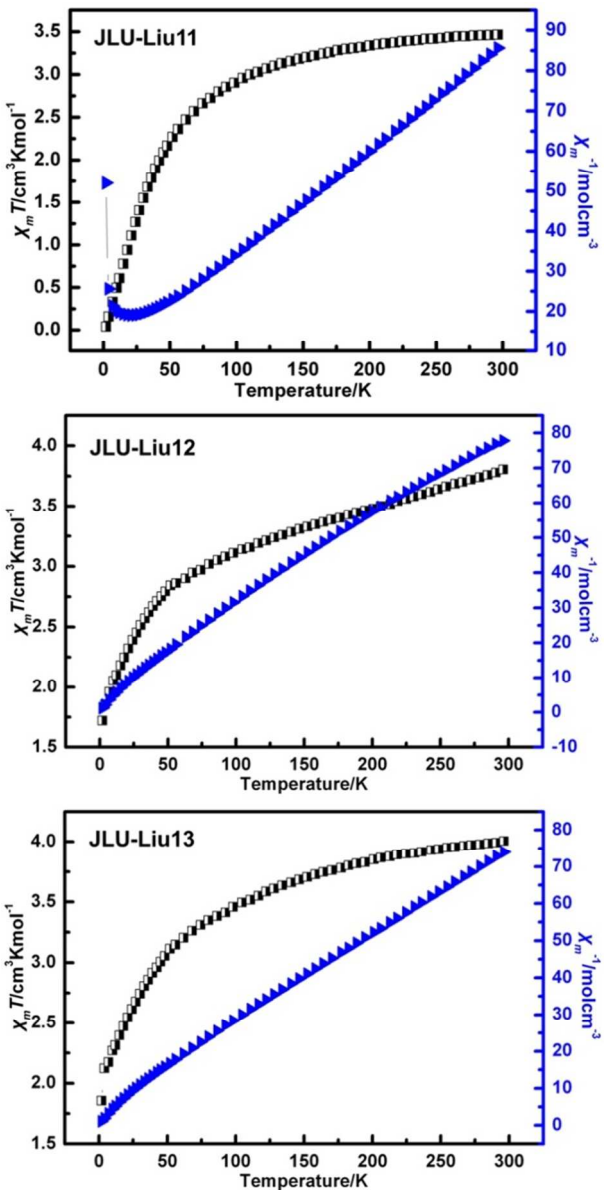

Fig. 9 Magnetic properties for **JLU-Liu11**, **JLU-Liu12** and **JLU-Liu13**.

Acknowledgements

The authors gratefully acknowledge the financial support of the Natural Science Foundation of China (Grant Nos. 21373095, 21371067 and 21171064).

Notes and references

[a] *State Key Laboratory of Inorganic Synthesis and Preparative Chemistry, College of Chemistry, Jilin University, Changchun 130012, P. R. China. E-mail: yunling@jlu.edu.cn; Fax: +86-431-85168624.*

[b] *Faculty of Chemistry and Material Science, Langfang Teachers College, Langfang, 065000, Hebei, P. R. China..*

†Electronic Supplementary Information (ESI) available: Selected bond lengths and angles, hydrogen bonding, additional figures for crystal structures, PXRD, IR and TGA. CCDC 1003340-1003342. For ESI and

crystallographic data in CIF or other electronic format see DOI: 10.1039/b000000x

1 (*a*) S.-T. Zheng, C. Mao, T. Wu, S. Lee, P. Feng and X. Bu, *J. Am. Chem. Soc*., 2012, **134**, 11936-11939; (*b*) R. Yun, Z. Lu, Y. Pan, X. You and J. Bai, *Angew. Chem., Int. Ed*., 2013, **52**, 11282-11285; (*c*) S.-T. Zheng, T. Wu, F. Zuo, C. Chou, P. Feng and X. Bu, *J. Am. Chem. Soc*., 2012, **134**, 1934-1937; (*d*) M. Li, D. Li, M. O'Keeffe and O. M. Yaghi, *Chem. Rev.*, 2014, **114**, 1343-1370.

2 (*a*) L. Ma, C. Abney and W. Lin, *Chem. Soc. Rev*., 2009, **38**, 1248-1256; (*b*) Z. Huang, P. S. White and M. Brookhart, *Nature*, 2010, **465**, 598-601; (*c*) F. Song, C. Wang, J. M. Falkowski, L. Ma and W. Lin, *J. Am. Chem. Soc*., 2010, **132**, 15390-15398.

3 C. Wang, T. Zhang and W. Lin, *Chem. Rev.*, 2012, **112**, 1084-1104.

4 (*a*) M. Kurmoo, *Chem. Soc. Rev*., 2009, **38**, 1353-1379; (*b*) G.-C. Xu, W. Zhang, X.-M. Ma, Y.-H. Chen, L. Zhang, H.-L. Cai, Z.-M. Wang, R.-G. Xiong and S. Gao, *J. Am. Chem. Soc*., 2011, **133**, 14948-14951; (*c*) W. Zhang and R.-G. Xiong, *Chem. Rev*., 2012, **112**, 1163-1195; (*d*) E. Coronado and G. Minguez Espallargas, *Chem. Soc. Rev*., 2013, **42**, 1525-1539.

5 (*a*) M. D. Allendorf, C. A. Bauer, R. K. Bhakta and R. J. T. Houk, *Chem. Soc. Rev*., 2009, **38**, 1330-1352; (*b*) Y. Cui, Y. Yue, G. Qian and B. Chen, *Chem. Rev*., 2012, **112**, 1126-1162; (*c*) Y. Cui, H. Xu, Y. Yue, Z. Guo, J. Yu, Z. Chen, J. Gao, Y. Yang, G. Qian and B. Chen, *J. Am. Chem. Soc*., 2012, **134**, 3979-3982.

6 (*a*) L. Lin, R. Yu, W. Yang, X.-Y. Wu and C.-Z. Lu, *Cryst. Growth Des*., 2012, **12**, 3304-3311; (*b*) C.-Y. Sun, X.-L. Wang, C. Qin, J.-L. Jin, Z.-M. Su, P. Huang and K.-Z. Shao, *Chem.–Eur. J*., 2013, **19**, 3639-3645; (*c*) Y. Wen, T. Sheng, S. Hu, X. Ma, C. Tan, Y. Wang, Z. Sun, Z. Xue and X. Wu, *Chem. Commun*., 2013, **49**, 10644-10646.

7 (*a*) L. E. Kreno, K. Leong, O. K. Farha, M. Allendorf, R. P. Van Duyne and J. T. Hupp, *Chem. Rev*., 2012, **112**, 1105-1125; (*b*) S. J. Butler and D. Parker, *Chem. Soc. Rev*., 2013, **42**, 1652-1666; (*c*) R.-B. Lin, F. Li, S.-Y. Liu, X.-L. Qi, J.-P. Zhang and X.-M. Chen, *Angew. Chem., Int. Ed*., 2013, **52**, 13429-13433.

8 (*a*) J.-R. Li, J. Sculley and H.-C. Zhou, *Chem. Rev*., 2012, **112**, 869-932; (*b*) Q. Yang, D. Liu, C. Zhong and J.-R. Li, *Chem. Rev*., 2013, **113**, 8261-8323; (*c*) J. Luo, J. Wang, G. Li, Q. Huo and Y. Liu, *Chem. Commun*., 2013, **49**, 11433-11435; (*d*) J. Pang, F. Jiang, M. Wu, D. Yuan, K. Zhou, J. Qian, K. Su and M. Hong, *Chem. Commun*., 2014, **50**, 2834-2836.

9 (*a*) M. Eddaoudi, J. Kim, N. Rosi, D. Vodak, J. Wachter, M. O'Keeffe and O. M. Yaghi, *Science*, 2002, **295**, 469-472; (*b*) S. Yang, X. Lin, W. Lewis, M. Suyetin, E. Bichoutskaia, J. E. Parker, C. C. Tang, D. R. Allan, P. J. Rizkallah, P. Hubberstey, N. R. Champness, K. Mark Thomas, A. J. Blake and M. Schröder, *Nat Mater*, 2012, **11**, 710-716; (*c*) T. Li, M. T. Kozlowski, E. A. Doud, M. N. Blakely and N. L. Rosi, *J. Am. Chem. Soc*., 2013, **135**, 11688-11691; (*d*) D.-X. Xue, A. J. Cairns, Y. Belmabkhout, L. Wojtas, Y. Liu, M. H. Alkordi and M. Eddaoudi, *J. Am. Chem. Soc*., 2013, **135**, 7660-7667.

10 (*a*) J.-R. Li, D. J. Timmons and H.-C. Zhou, *J. Am. Chem. Soc*., 2009, **131**, 6368-6369; (*b*) Y. Kang and F. Wang, *CrystEngComm*, 2014, **16**, 4088-4090; (*c*) T. Li, J. Yang, X.-J. Hong, Y.-J. Ou, Z.-G. Gu and Y.-P. Cai, *CrystEngComm*, 2014, **16**, 3848-3852.

11 (*a*) H. Wang, F.-Y. Yi, S. Dang, W.-G. Tian and Z.-M. Sun, *Cryst. Growth Des*., 2013, **14**, 147-156; (*b*) S. I. Vasylevs'kyy, G. A. Senchyk, A. B. Lysenko, E. B. Rusanov, A. N. Chernega, J. Jezierska, H. Krautscheid, K. V. Domasevitch and A. Ozarowski, *Inorg. Chem.*, 2014, **53**, 3642-3654.

12 (*a*) F. A. Almeida Paz, J. Klinowski, S. M. F. Vilela, J. P. C. Tome, J. A. S. Cavaleiro and J. Rocha, *Chem. Soc. Rev*., 2012, **41**, 1088-1110; (*b*) T. R. Cook, Y.-R. Zheng and P. J. Stang, *Chem. Rev*., 2013, **113**, 734-777; (*c*) T. A. Makal, X. Wang and H.-C. Zhou, *Cryst. Growth Des*., 2013, **13**, 4760-4768.

13 (*a*) E. D. Bloch, D. Britt, C. Lee, C. J. Doonan, F. J. Uribe-Romo, H. Furukawa, J. R. Long and O. M. Yaghi, *J. Am. Chem. Soc*., 2010, **132**, 14382-14384; (*b*) S. Huh, S. Jung, Y. Kim, S.-J. Kim and S. Park, *Dalton Trans*., 2010, **39**, 1261-1265; (*c*) L. Shen, D. Gray, R. I. Masel and G. S. Girolami, *CrystEngComm*, 2012, **14**, 5145-5147; (*d*) M. Gustafsson, J. Su, H. Yue, Q. Yao and X. Zou, *Cryst. Growth Des*., 2012, **12**, 3243-3249; (*e*) C. Wang, Z. Xie, K. E. deKrafft and W. Lin, *J. Am. Chem. Soc*., 2011, **133**, 13445-13454; (*f*) C. Wang, K. E. deKrafft and W. Lin, *J. Am. Chem. Soc*., 2012, **134**, 7211-7214; (*g*) C. A. Kent, D. Liu, T. J. Meyer and W. Lin, *J. Am. Chem. Soc*., 2012, **134**, 3991-3994; (*h*) J. Wang, J. Luo, J. Zhao, D.-S. Li, G. Li, Q. Huo and Y. Liu, *Cryst. Growth Des*., 2014, **14**, 2375-2380; (*i*) J. Wang, J. Luo, B. Zhi, G. Li, Q. Huo and Y. Liu, *CrystEngComm*, 2014, **16**, 9810-9816.

14 (*a*) X. Jing, L. Zhang, T. Ma, G. Li, Y. Yu, Q. Huo, M. Eddaoudi and Y. Liu, *Cryst. Growth Des.*, 2009, **10**, 492-494; (*b*) S.-L. Cai, S.-R. Zheng, Z.-Z. Wen, J. Fan and W.-G. Zhang, *Cryst. Growth Des*., 2012, **12**, 2355-2361.

15 G. M. Sheldrick, SHELXTL-97, Program for Crystal Structure Refinement, University of Gottingen, 1997.

16 V. S. A. Blatov, V. Serezhkin and D. Korchagin, http://www.topos.ssu.samara.ru.

17 B. Liu, Y. Li, L. Hou, G. Yang, Y.-Y. Wang and Q.-Z. Shi, *J. Mater. Chem. A*., 2013, **1**, 6535-6538.

18 (*a*) W. Lin, M. E. Chapman, Z. Wang and G. T. Yee, *Inorg. Chem*., 2000, **39**, 4169-4173; (*b*) S.-i. Noro, S. Kitagawa, T. Nakamura and T. Wada, *Inorg. Chem*., 2005, **44**, 3960-3971; (*c*) C.-G. Zheng, Y.-L. Xie, R.-G. Xiong and X.-Z. You, *Inorg. Chem. Commun*., 2001, **4**, 405-408.

19 A. L. Spek, J. Appl. Crystallogr., 2003, **36**, 7-13.

Structural diversity and magnetic properties of three metal−organic frameworks assembled from a T-shaped linker

Jing Wang,[a] Xuemin Jing,[b] Yu Cao,[a] Guanghua Li,[a] Qisheng Huo[a] and Yunling Liu*[a]

Three helical metal-organic frameworks have been solvothermally synthesized by reacting a T-shaped linker, 2,2′-bipyridyl-5,5′-dicarboxylic acid (H_2bpydc) ligand with transition metals. Additionally, the magnetic properties of all compounds have been studied.